Journal of Alloys and Compounds 509 (2011) 9264–9270

Contents lists available at ScienceDirect

Journal of Alloys and Compounds

journal homepage: www.elsevier.com/locate/jallcom

Influences on photovoltage performance by interfacial modification of FTO/mesoporous TiO_2 using ZnO and TiO_2 as the compact film

Yumin Liu[a], Xiaohua Sun[a], Qidong Tai[a], Hao Hu[a], Bolei Chen[a], Niu Huang[a], Bobby Sebo[a], Xing-Zhong Zhao[b,*]

[a] School of Physics and Technology, Wuhan University, Wuhan 430072, People's Republic of China
[b] School of Physics and Technology, Key Laboratory of Artificial Micro- and Nano-structures of Ministry of Education, Wuhan University, Wuhan 430072, People's Republic of China

ARTICLE INFO

Article history:
Received 7 May 2011
Received in revised form 7 July 2011
Accepted 8 July 2011
Available online 18 July 2011

Keywords:
Zinc oxide compact film
Energy barrier
Electron density
Dye-sensitized solar cell
Photovoltage performance

ABSTRACT

An effective ZnO compact film (ZCF) has been introduced at the interface of fluorine doped tin oxide (FTO) substrate and mesoporous TiO_2 layer, and its effect on dye-sensitized solar cells (DSSCs) has been compared to that of conventional TiO_2 compact film (TCF). The ZCF and TCF prepared by spin-coating method on FTO are characterized by energy-dispersive X-ray spectroscopy (EDX), scanning electron microscopy (SEM), and UV–vis spectrophotometer. The existence of TiO_2 can suppress the recombination occurring at the interface of FTO/electrolyte, resulting in a higher J_{sc} and V_{oc} than bare FTO. The ZCF creates an energy barrier between FTO substrate and mesoporous TiO_2 layer, which not only reduces the electron back transfer from FTO to I_3^- in the electrolyte, but also leads to the accumulation of photogenerated electrons, and increases the electron density in the conduction band of TiO_2. The device based on FTO/ZCF substrate remarkably improves V_{oc} and FF, finally increases energy conversion efficiency by 13.1% compared to the device based on bare FTO and 4.7% compared to the counterpart based on FTO/TCF.

1. Introduction

Since O'Regan et al. reported their breakthrough discovery in 1991 [1], dye-sensitized solar cells (DSSCs) based on nanocrystalline TiO_2 have attracted extensive attentions in academic research and industrial applications. Owing to the low cost and high efficiencies, DSSCs may offer an alternative to conventional semiconductor-based solar cells. A typical DSSC consists of a mesoporous nanocrystalline TiO_2 film covered by a monolayer of dye molecules, electrolyte, and counterelectrode. Recently, intensive efforts have been carried out to modify the interfaces of each part to improve the photoelectrochemical performance. For example, Au [2], ZnO [3,4], MgO [5,6], and Al_2O_3 [7,8] have been introduced to modify the surface of mesoporous TiO_2 electrode, which mainly focuses on decreasing the interfacial charge recombination via forming an energy barrier between TiO_2 electrode and electrolyte. In addition, many efforts have been made to investigate the interface of electrode/dye [9,10] and dye/electrolyte [11] to optimize interfacial dynamics. On the other hand, a few groups have studied the interface of conducting glass/TiO_2 mainly to investigate its effect on the performance of DSSCs by employing a compact film [12–14]. However, research on this important interface is not intense as compared to modification of the others.

It is essential to introduce an efficient compact film to FTO glass surface to reduce the charge recombination between electrons emanating from FTO substrate and I_3^- ions present in electrolyte. Zhu et al. [15] reported that recombination occurs predominantly in the region of fluorine doped tin oxide (FTO) substrate rather than homogeneously across the depth of the TiO_2 film based on the results from Intensity-Modulated Infrared Spectroscopy (IMIS) analysis. In the past decade, a majority of researches employed TiO_2 as the compact film on the interface of FTO/TiO_2 [16–18], and it has been found that the influence of TiO_2 compact layer is extremely relevant for the determination of DSSCs performance. It has been reported by Xia et al. [19,20] that an effective Nb_2O_5 compact film was introduced by sputtering method to create a potential barrier between the FTO substrate and TiO_2, which improved open-circuit photovoltage and fill factor, and kept short-circuit photocurrent density (J_{sc}) virtually unchanged by controlling the thickness of Nb_2O_5 layer. Recently, Nb doped-TiO_2 (NTO) thin film was deposited on FTO substrate to form a compact film for DSSCs by pulsed laser deposition (PLD), which achieved an obvious effect [21,22]. Nevertheless, Nb_2O_5 and NTO are expensive materials for compact film, and the methods of sputtering or PLD may not be the best choice for industrialization due to the high cost of manufacturing process. On the other hand, it is revelatory for us to suppose that a methodology of introducing an energy barrier at FTO/TiO_2

* Corresponding author. Tel.: +86 27 87642784; fax: +86 27 87642569.
E-mail address: xzzhao@whu.edu.cn (X.-Z. Zhao).

0925-8388/$ – see front matter © 2011 Elsevier B.V. All rights reserved.
doi:10.1016/j.jallcom.2011.07.018

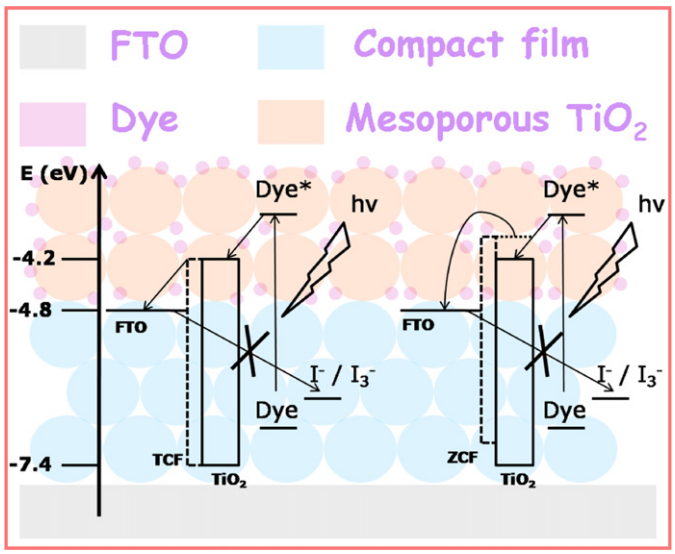

Fig. 1. Schematic view of the electron transfer with TCF and ZCF layers.

interface rather than the surface of TiO_2 electrode may be more feasible.

Due to its stability against photocorrosion and photochemical properties, ZnO has been widely investigated for the application on dye-sensitized solar cells [23–25]. In our previous work [26], we first developed ZnO by a facile spin-coating method as compact film at FTO/TiO_2 interface with an enhanced performance (improvement of V_{oc}, fill factor, and energy conversion efficiency). We have systematically investigated the thickness effect of ZnO compact film (ZCF) to electrochemical performance. However, to our best knowledge, the different mechanism of ZCF to photoelectron conversion process have not been reported, comparing with conventional TiO_2 compact film (TCF).

In this work, we introduced ZnO as the compact film at FTO/TiO_2 interface, which mainly plays the role of creating an energy barrier between FTO substrate and mesoporous TiO_2 layer. This potential barrier will lead to the following two effects to charge transport at the interface of FTO and TiO_2: (a) suppressing back electrons transfer from FTO to electrolyte and (b) blocking the electrons injection from the conduction band of TiO_2 to FTO which would further affects the electron density in TiO_2. The latter effect does not exist in the condition of employing TiO_2 as the compact film. The schematic view of electron transfer with ZCF and TCF is shown in Fig. 1. We report here the details of fabrication and characterization of ZnO compact film (ZCF) and TiO_2 compact film (TCF). Furthermore, we investigated their different influences to photoelectron conversion process and the performance of DSSC in the same condition, which have been supported by the results from current–voltage characteristics, open-circuit voltage decay (OCVD) technique and electrochemical impedance spectroscopy (EIS) analysis of the devices.

2. Experimental details

2.1. Materials

Poly (ethylene glycol) (PEG, MW = 20 000), Triton-X100, Zinc acetate, diethanolamine (DEA), tetrabutyl titanate (TBT), HNO_3, CH_3COOH, and propylene carbonate (PC) were obtained from Sinopharm Chemical Reagent Corporation (China). Lithium iodide (LiI, 99%), 4-*tert*-butylpyridine (TBP), guanidinium thiocyanate (GNCS) and titanium tetraisopropoxide (98%) were purchased from Acros. Iodine (I_2, 99.8%) was obtained from Beijing Yili chemicals (China). The Ru dye, *cis*-di(thiocyanato)-bis(2,2′-bipyridyl-4,4′-dicarboxylate) ruthenium(II) (N719), were purchased from Solaronix (Switzerland). All the reagents used were of analytical purity. Fluorine-doped SnO_2 conductive glass (FTO, sheet resistance 10–15 $\Omega\,sq^{-1}$, Asahi Glass, Japan) were used as the substrate for spin-coating ZCF and TCF.

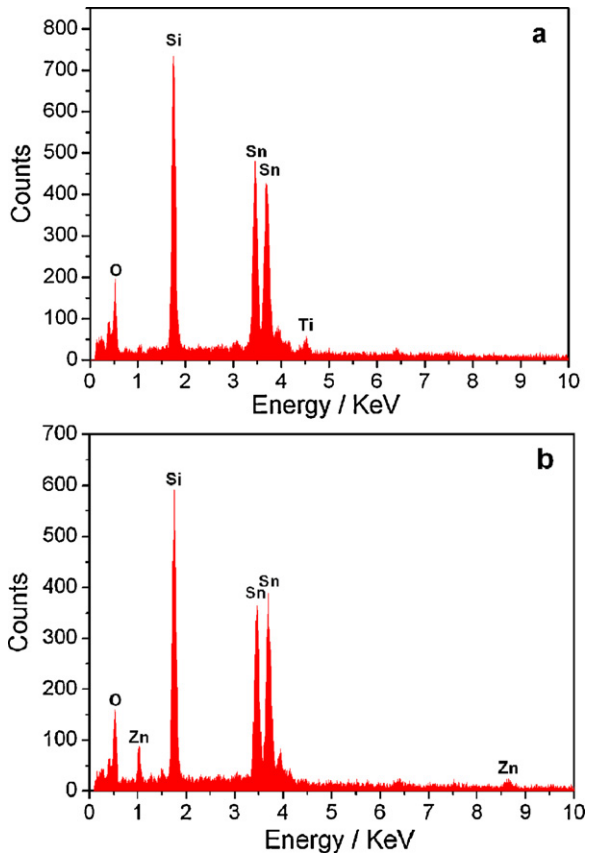

Fig. 2. EDX spectra for (a) FTO/TCF and (b) FTO/ZCF substrates.

2.2. Preparation and characterization of ZnO and TiO_2 compact films

ZnO sol was prepared according to previous publication [27]. Firstly, 1.84 g Zinc acetate was added into 50 ml of absolute ethanol under stirring (50 °C). When the solution changed into a white emulsion, an amount of DEA was added into the emulsion, the molar ratio of DEA/Zinc acetate being 1:1. The emulsion then became clear immediately. After stirring for about 10 min, the content became a steady homogeneous sol without any precipitation. TiO_2 sol was fabricated as the following process. Firstly, 3.4 ml tetrabutyl titanate and 0.8 ml diethanolamine were dissolved in 40 ml ethanol and stirred vigorously for 1 h at 40 °C until a homogeneous solution was formed. A mixture of 0.2 ml H_2O and 9 ml ethanol was added dropwise into the formed solution under rapid stirring. Then the resulting solution, aged for 24 h at room temperature, resulted in a TiO_2 sol.

To investigate the effects of ZnO and TiO_2 compact films on the performance of DSSCs, spin-coating method was applied to coat forementioned ZnO and TiO_2 sols at the same concentration (0.2 M) on clean FTO substrates. The coating films were dried in air for 30 min, and then sintered at 500 °C for an hour to form ZnO and TiO_2 compact films, the thickness of two compact films is controlled as about 150 nm.

Energy-dispersive X-ray spectroscopy (EDX, GENESIS 7000) was used to determine the chemical species of the composite substrates. The surface morphology of ZnO and TiO_2 compact films was observed by scanning electron microscopy (SEM, Sirion FEG, USA). UV–vis adsorption spectra were recorded on a UV–vis–NIR spectrophotometer (Cary 5000, Varian).

2.3. Device fabrication and measurements

Mesoporous nanocrystalline TiO_2 film was fabricated with a colloid, which were prepared by the hydrolysis of titanium tetraisopropoxide according to the reported procedure [28], by a doctor-blading technique. The edges of conducting glass were covered with adhesive tapes as the frame. The concentration of TiO_2 colloids and the layer numbers of tapes are same to make the TiO_2 films with same thickness. The TiO_2 colloids was spread on bare FTO, FTO/TCF and FTO/ZCF substrates, followed by sintering at 500 °C for 30 min. The thickness of mesoporous TiO_2 film was 10 μm, as measured with a TalyForm S4C-3D profilometer (UK). The mesoporous TiO_2 electrode was preheated at 120 °C for 20 min, and then immersed into the solution of *cis*-di(thiocyanato)-bis(2,2′-bipyridyl-4,4′-dicarboxylate) ruthenium(II) with a concentration of 500 μM in the mixture of acetonitrile and *tert*-butyl alcohol (volume ratio: 1/1) at 60 °C for 12 h. Then the electrodes were washed with acetonitrile to remove the accumulated dye molecules on the surface of

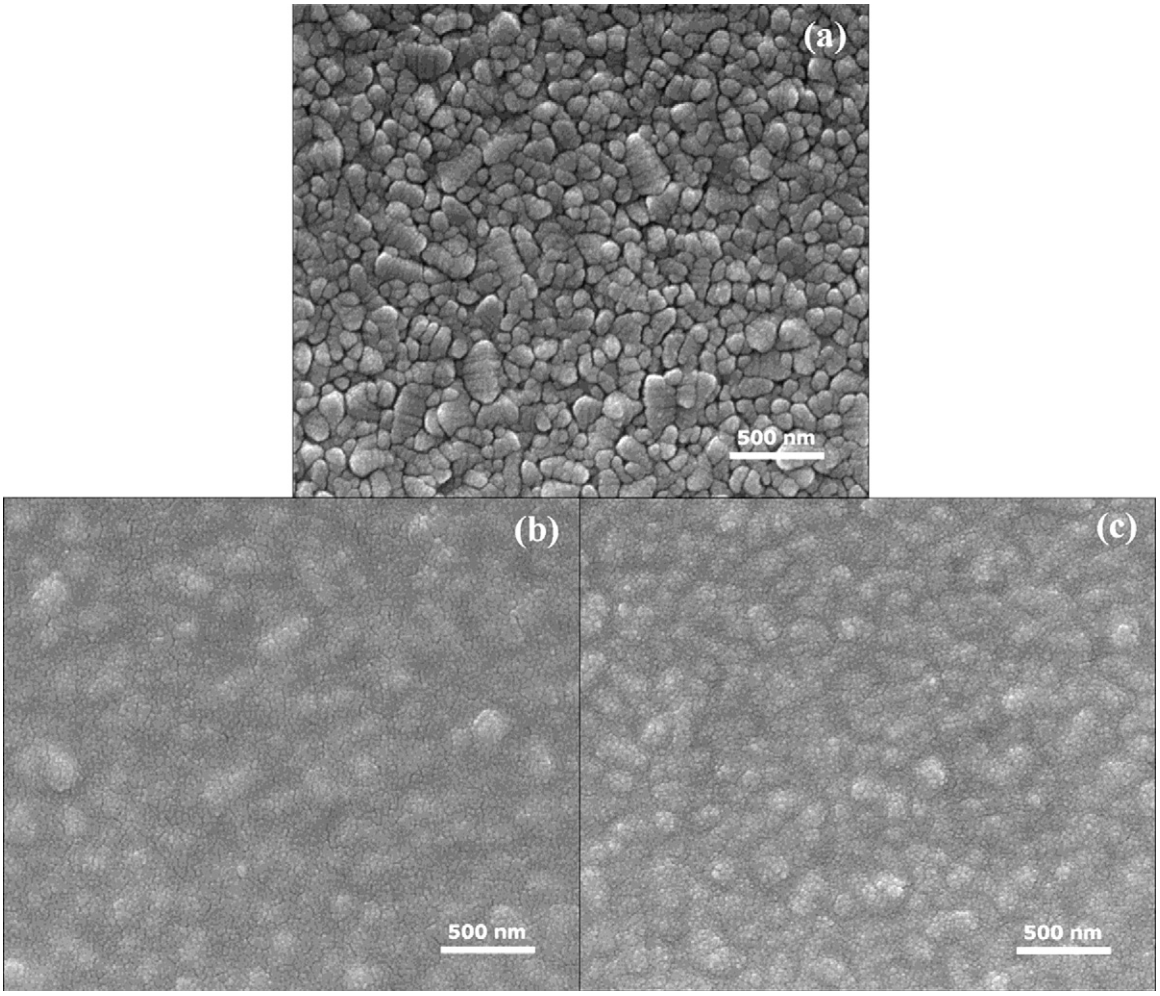

Fig. 3. Scanning electron micrograph of the surface morphology of (a) bare FTO, (b) TiO_2 compact film (TCF) and (c) ZnO compact film (ZCF) after calcinations at 500 °C.

nanocrystalline TiO_2 to ensure that the film was covered with a monolayer of dye molecules. A sandwich-type DSSC configuration was fabricated by assembling the dye-loaded mesoporous TiO_2 with platinum plate counter electrode. The assembled cell was then clipped together as an open cell. An electrolyte composed of 0.1 M 1-propy-3-methylimidazolium iodide (PMII), 0.05 M LiI, 0.1 M GNCS, 0.03 M I_2, 0.5 M 4-*tert*-butylpridine (TBP) in mixed solvent of acetonitrile and propylene carbonate (PC) (volume ratio: 1/1) was injected into the open cell from the edges, and then the cell was tested immediately.

A 500 W xenon light source (Oriel 91192, USA) was used to give an irradiance of 90.4 mW cm^{-2} (AM 1.5, global) which was calibrated by a Si-1787 photodiode (spectral response range: 320–730 nm). The current–voltage characteristics of the cells were recorded by applying external potential bias to the device and measuring the generated photocurrent with a source meter (model 2400, Keithly Instruments Inc., USA). The irradiated area of each cell was kept as 0.25 cm^2 by using a light tight metal mask for all samples. Impedance measurements were performed with a computer-controlled electrochemical workstation (CHI660C, CH Instruments) under the bias voltage of V_{oc} in the illumination. The frequency range was 0.05–100 kHz and the magnitude of modulation signal was 0.01 V.

3. Results and discussion

To confirm the formation of ZnO and TiO_2 on FTO substrates, an EDX measurement was carried out. As shown in Fig. 2(a) and (b), we can clearly distinguish the peak position of zinc and titanium from others, respectively, which are Sn, Si, O. Those are the composition of FTO. Fig. 3 shows the SEM surface morphology of bare FTO, FTO/TCF, and FTO/ZCF substrates. The bare FTO surface shows characteristic morphology of tin oxide crystals (Fig. 3a), in which particle size is around 100–400 nm. After spin-coating ZCF and TCF, we can observe that both of the substrates were covered with small particles, which were homogeneously distributed on FTO surface, as shown in Fig. 3(b) and (c). Based on the characterization of SEM, we can confirm that the two compact films successfully prevented the physical contact of FTO and mesoporous TiO_2.

In addition, it is necessary for us to investigate the optical properties of the substrates after introducing the compact film, since the

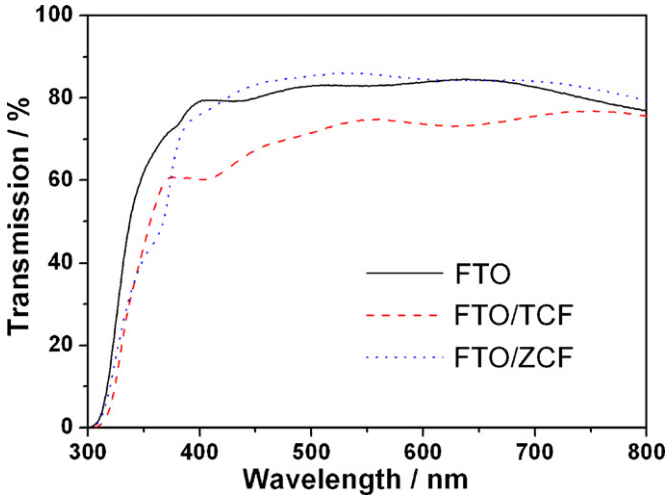

Fig. 4. UV-spectra of bare FTO, FTO/TCF and FTO/ZCF substrates.

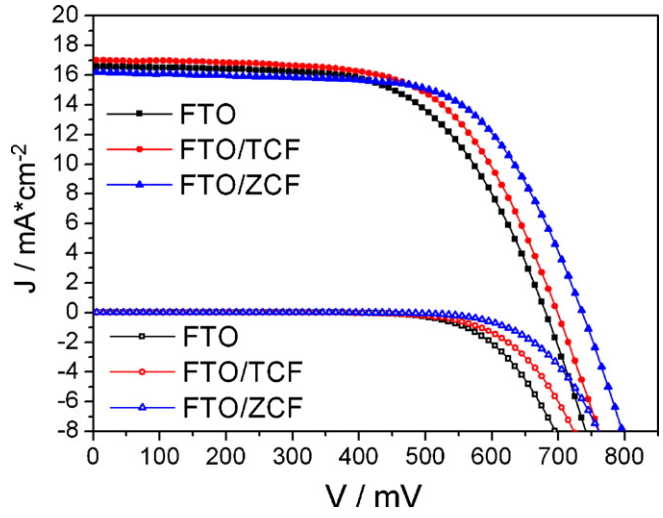

Fig. 5. Photocurrent density–voltage characteristics of DSSCs based on bare FTO, FTO/TCF and FTO/ZCF substrates. Solid symbols were measured under AM 1.5 irradiation of 90.4 mW cm^{-2}. Open symbols were measured in the dark.

devices were illuminated from FTO substrate side in working condition. Fig. 4 shows the UV-spectra of bare FTO, FTO/TCF, and FTO/ZCF substrates. In the region from 400 nm to 800 nm, the transmission of FTO/ZCF do not change almost compared with those of bare FTO substrate, which implies that ZCF will not influence the harvest of light in the most of the visible region. Though, the transmission obviously decreases in the region from 300 nm to 400 nm, the optical properties of FTO/ZCF are more applicable for DSSCs than FTO/TCF substrate. Since the transmission of FTO/ZCF is higher than that of FTO/TCF substrate in the whole region of visible light.

Fig. 5 presents the photocurrent density–voltage characteristics of DSSCs employing bare FTO, FTO/TCF, and FTO/ZCF substrates at an irradiance of AM 1.5 sunlight (90.4 mW cm^{-2}). And detailed photovoltaic performance parameters of DSSCs with different substrates are listed in Table 1. The short-circuit photocurrent density (J_{sc}), open-circuit voltage (V_{oc}) and fill factor (FF) of device based on bare FTO were 16.55 mA cm^{-2}, 681.03 mV and 0.61, respectively, corresponding to an energy conversion efficiency of 6.86%. The device based on FTO/TCF gave an improvement of V_{oc} about 20 mV and J_{sc} increased slightly (from 16.55 to 17.02 mA cm^{-2}), finally resulting in a higher energy conversion efficient 7.41% compared with the counterpart based on bare FTO substrate. The increase in J_{sc} and V_{oc} of DSSC incorporating TiO_2 compact film can be ascribed to the reduced charge recombination by suppressing back electrons transfer from FTO to electrolyte [29]. In the case of employing ZnO as the compact film, the device gave improvement in V_{oc} by 8.1% (from 681.03 to 736.14 mV) and FF (from 0.61 to 0.65), while J_{sc} decreased to some extent, finally resulting in an energy conversion efficiency of 7.76% which was enhanced by 13.1% compared to the device based on bare FTO and 4.7% compared to the counterpart based on FTO/TCF substrate. It shows the merits of introducing ZnO at FTO/TiO_2 interface by spin-coating method compared with the conventional TiO_2 compact film. The different effects to the photoelectron conversion process by employing ZnO and TiO_2 as the compact film and the detailed mechanism of improving the performance of DSSCs were mainly discussed below.

To investigate the effects of TCF and ZCF of suppressing back electrons transfer from FTO to electrolytes, the photocurrent density–voltage characteristics were also measured in the dark. As can be seen in Fig. 5, the onset of the dark current density was shifted by a few hundred millivolts for the devices based on FTO/ZCF and FTO/TCF, and the current of FTO/ZCF and FTO/TCF increased much slower than that of bare FTO. In addition, the dark current of device based on FTO/ZCF was much less than that of the counterpart employing FTO/TCF substrate, because the conduction band edge of ZnO is more negative than TiO_2 which lead to stronger blocking effect for the back transfer of electrons. The reduction of the dark current demonstrates that the two compact films successfully reduced the reaction sites for the charge recombination between electrons emanating from the FTO substrate and I_3^- ions present in the electrolyte [26], and implies that ZnO is a suitable and superior material for the compact layer in DSSCs than the conventional TiO_2.

Electrochemical impedance spectroscopy (EIS) analysis has been widely employed to investigate the electron-transport and recombination in DSSCs. To further characterize the different kinetics of electrochemical progress occurring in DSSCs based on FTO/TCF and FTO/ZCF substrates, the electrochemical impedance spectroscopy of corresponding devices were measured in the illumination with the bias voltage of V_{oc}. Fig. 6(a) shows Nyquist plots of DSSCs based on bare FTO, FTO/TCF, and FTO/ZCF substrates. The impedance components of the interfaces in DSSCs observed in the frequency regions of 10^3–10^5 Hz (ω_1), 1–10^3 Hz (ω_2), 0.1–1 Hz (ω_3) are associated with the charge transport at the FTO/TiO_2 and Pt counter electrode/electrolyte interfaces (Z_1), the TiO_2/dye/electrolyte interfaces (Z_2), and the Nernstian diffusion in the electrolyte (Z_3), respectively [30,31]. Table 2 summarized the results of EIS analysis fitted by an equivalent circuit containing a constant phase element (CPE) and resistance (R) (Fig. 6a, inset). The resistance of the Z_1 component (R_1) is given by the sum of resistances of counter electrode/electrolyte and FTO/TiO_2 interfaces [32]. As shown in Fig. 6(a) and Table 2, it is noted that the value of R_1 does not change almost after introducing TiO_2 as the compact film, whereas it increased observably in the case of employing FTO/ZCF substrate (from 2.29 to 3.46 Ω). Since an identical Pt counter electrode was employed for all the devices, the noticeable difference at the interface of FTO/TiO_2 is wholly responsible for the value of R_1. The increment of R_1 implies that the existence of ZnO compact film increases the interfacial resistance between FTO and mesoporous TiO_2, since the conduction band edge of ZnO is more negative than that of TiO_2, which results in the formation of an energy barrier at the interface of FTO/TiO_2. This energy barrier will retard the electrons injected from the conduction band of TiO_2 to FTO, so the short-circuit photocurrent density (J_{sc}) of DSSCs based on FTO/ZCF substrate decreased compared to that of bare FTO, which was in good agreement with the previous photocurrent density–voltage characteristics. As a consequence, the photogenerated electrons will accumulate in the conduction band of TiO_2, which led to the increment of electron density in TiO_2, and thus the shift upward of Fermi level for electrons in the TiO_2 electrode. In general, the open-circuit voltage (V_{oc}) value of a DSSC is defined as the difference in energy between Fermi level of the photoelectrode semiconductor

Table 1
Photovoltaic properties of dye-sensitized solar cells based on: the bare FTO, FTO/TCF, and FTO/ZCF substrates[a].

Sample	J_{sc} (mA cm^{-2})	V_{oc} (mV)	FF	Eff. (%)
FTO	16.55	681.03	0.61	6.86
FTO/TCF	17.02	700.04	0.62	7.41
FTO/ZCF	16.21	736.14	0.65	7.76

[a]The parameters were tested under AM 1.5 full sunlight (100 mW cm^{-2}).

Table 2
Fitting results of EIS analysis.

Sample	R_1 (Ω)	R_2 (Ω)	ω_{max} of Z_2 (Hz)
FTO	2.29	22.34	4.92
FTO/TCF	2.38	21.49	4.54
FTO/ZCF	3.46	17.72	5.18

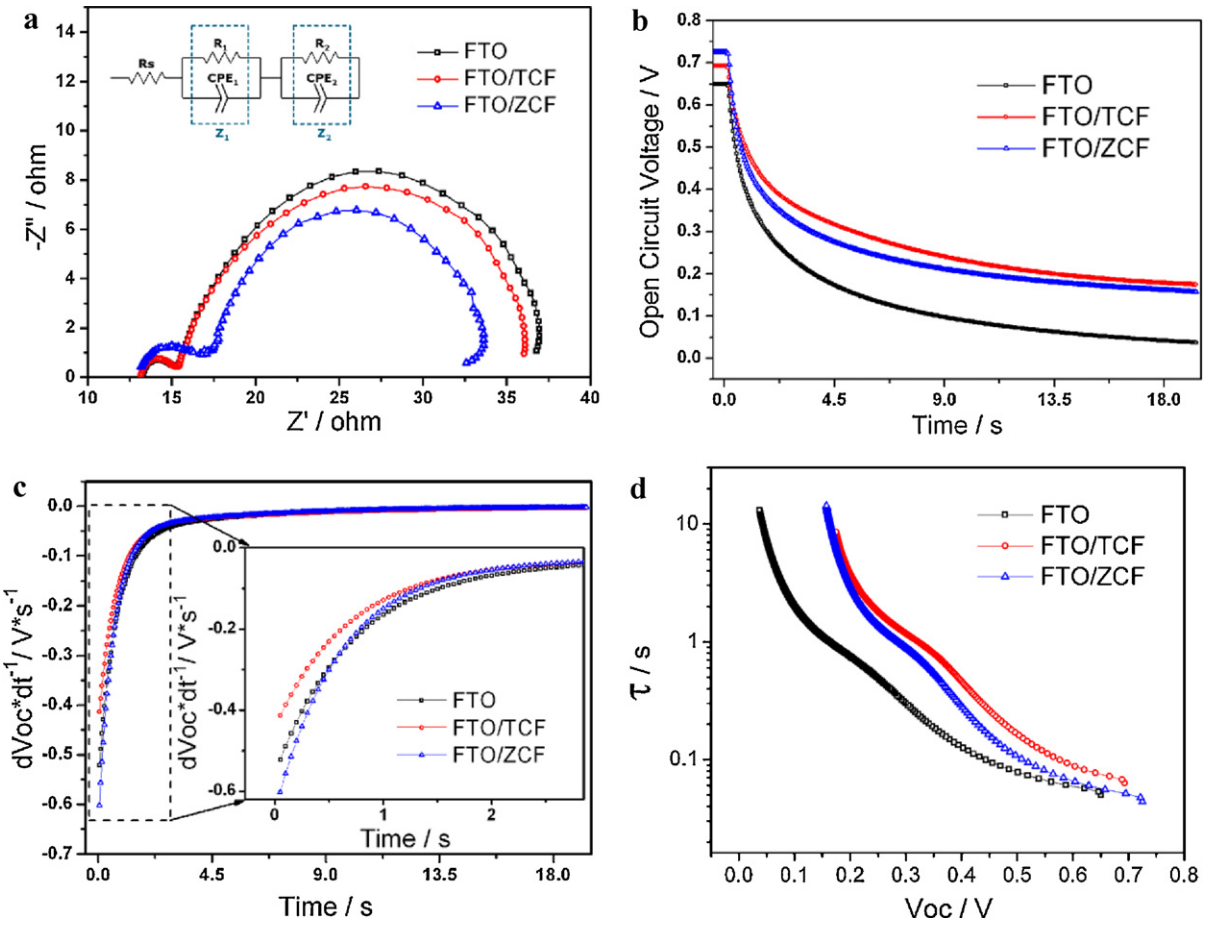

Fig. 6. (a) Nyquist plots of DSSCs based on bare FTO, FTO/TCF and FTO/ZCF substrates. The impedance spectra were measured in the illumination with the bias voltage of V_{oc}. The inset shows the equivalent circuit. (b) Open circuit potential decay for the DSSCs based on bare FTO, FTO/TCF and FTO/ZCF substrates. (c) Dependence of the rate of open-circuit voltage decay ($dV_{oc}\,dt^{-1}$) on time based on different substrates: bare FTO, FTO/TCF and FTO/ZCF substrates. (d) Electron lifetime (in log-linear representation) as a function of open-circuit voltage (V_{oc}) for DSSCs based on different substrates: bare FTO, FTO/TCF and FTO/ZCF substrates.

oxide and the redox potential of the electrolyte [33,34]. Therefore, the rise of Fermi level resulting from the increase of electron density in the conduction band of TiO_2 will improve the V_{oc} remarkably, which has been demonstrated by the photocurrent density–voltage characteristics. However, this energy barrier does not exist in the case of employing TiO_2 as the compact film, which lead to the same value of R_1 compared to the device based on bare FTO substrate. So there was no blocking effect for electrons injected from the conduction band of TiO_2 to FTO. J_{sc} and V_{oc} of the device based on FTO/TCF substrate increased mainly due to the reduced charge recombination by suppressing back electrons transfer from FTO to electrolyte. In addition, R_2, the resistance of interfacial charge-transfer from the conduction band of TiO_2 to triiodide in the electrolyte, decreases due to the increase of electron density in TiO_2 [35,36]. As shown in Table 2, R_2 of DSSCs based on bare FTO, FTO/TCF, and FTO/ZCF substrates were 22.34 Ω, 21.49 Ω, and 17.72 Ω, respectively, which also demonstrated the notable increase of electron density in the conduction band of TiO_2 after introducing ZnO as the compact film. On the other hand, the electron lifetime in TiO_2 is inversely proportional to the frequency of maximum Z'' at the Z_2 component (ω_{max}) [37].

$$\tau = \frac{1}{\omega_{max}} \tag{1}$$

As can be seen in Table 2, ω_{max} of the devices based on bare FTO, FTO/TCF, and FTO/ZCF substrates were 4.92 Hz, 4.54 Hz, and 5.18 Hz, respectively. Therefore, we can conclude that the electron lifetime was increased in the presence of TiO_2 compact film, which was consistent with the previous reports [21], whereas decreased after introducing ZnO compact film. The latter result was seldom reported in the past.

In order to explore the origin of electron lifetime decreasing in the case of employing ZnO as the compact film, while on the contrary in the presence of TCF, open-circuit voltage decay (OCVD) characteristics of devices based on bare FTO, FTO/TCF, and FTO/ZCF substrates were measured. OCVD is a technique which monitor the subsequent decay of photovoltage (V_{oc}) after turning off the illumination in a steady state [38]. The decay of photovoltage reflects the decrease of electron density in the conduction band of TiO_2, which is mainly caused by the charge recombination occurring at FTO/electrolyte and TiO_2/electrolyte interfaces. In other words, the recombination rate of photoelectron is proportional to the rate of photovoltage decay. As shown in Fig. 6(b), it is obvious that the value of photovoltage response of devices based on FTO/TCF and FTO/ZCF substrates was higher than that of bare FTO in the whole time region. This demonstrates that the two compact films suppressed the recombination pathway occurring at the interface of FTO and electrolyte effectively. Then we calculated the rate of open-circuit voltage decay ($dV_{oc}\,dt^{-1}$) obtained from the data shown in Fig. 6(c), which is inversely proportional to the electron lifetime as reported by others [38,39].

$$\tau = \frac{k_B T}{e}\left(\frac{dV_{oc}}{dt}\right)^{-1} \tag{2}$$

One should pay close attention to the start point of the curve shown the dependence of $dV_{oc}\,dt^{-1}$ on the time in Fig. 6(c), since the onset for the curve mainly reflects the recombination rate of photoelectron of the device in illumination corresponding to a high electron density. In the short time region, we can see that the absolute value of $dV_{oc}\,dt^{-1}$ based on FTO/ZCF was higher to bare FTO substrate, the counterpart based on FTO/TCF was lower, which implies the recombination rate of devices based on different substrates in the order FTO/ZCF > bare FTO > FTO/TCF in illumination. The mesoporous TiO_2 films were prepared by identical fabrication procedure, so the density of recombination center and bulk traps inside the TiO_2 electrode for each sample was the same. Consequently, the different recombination rates of the samples were mainly related to the difference at the interface of FTO and mesoporous TiO_2. The increment of electron density which due to introducing ZnO as the compact film increased the possibility of recombination of the photoelectron by reaction with I_3^- ions present in the electrolyte, resulting in the highest recombination rate among the samples, and leading to the decrease of electron lifetime. However, the existence of TiO_2 mainly prevented the physical contact of FTO and electrolyte, which only suppressed the recombination occurring at the interface of FTO/electrolyte, without any blocking effect for electrons transfer from the conduction band of TiO_2 to FTO. Therefore, the device employing FTO/TCF substrate resulted in the lowest recombination rate. From the foregoing discussion, we can derive the electron lifetime of samples employing different substrates in illumination in the order FTO/TCF > bare FTO > FTO/ZCF which was in good agreement with the results of EIS analysis. In addition, the absolute value of $dV_{oc}\,dt^{-1}$ of the device based on FTO/ZCF substrate was inferior to that of bare FTO after 0.5 s, which means that the recombination rate reduced after the electron density of the sample decayed to a normal level, since the effect of suppressing recombination occurring at the interface of FTO/electrolyte was primary in this condition. And the same results can be obtained from Fig. 6(d), which plotted the electron lifetime (in log-linear representation) as a function of V_{oc} by Eq. (2).

The fill factor is a measurement which reflects the increase in recombination or decrease in photocurrent with increasing photovoltage [40]. If the electron transfer rate from TiO_2 to the triiodide increases, the potential of the TiO_2 will become less negative for the decrease of the electron density in the conduction band of TiO_2, which results in the low fill factor. Therefore, the device based on FTO/TCF substrate achieved a higher FF than that based on bare FTO for the reason of reducing the loss of photoelectron by suppressing the recombination occurring at the interface of FTO/electrolyte. Based on the above discussion, the recombination rate of photoelectron increased after introducing ZnO as the compact film, however, we obtained a remarkable increment of the electron density in the conduction band of TiO_2, which leads that the potential of TiO_2 becomes more negative, and so the highest fill factor.

4. Conclusions

In summary, we have successfully introduced ZnO as an effective compact film, which greatly enhanced V_{oc} and FF with compensation of J_{sc} decrease, finally increasing energy conversion efficiency of DSSCs. Furthermore, different influences on photoelectron conversion process and DSSC performance by employing ZCF and TCF have been investigated. We found that the existence of TCF mainly prevented the physical contact of FTO and electrolyte, which only suppressed the recombination occurring at the interface of FTO/electrolyte, without any blocking effect for electrons transfer from the conduction band of TiO_2 to FTO. So J_{sc} and V_{oc} of the device based on FTO/TCF substrate were higher than those of the counterpart employing bare FTO. However, the ZCF created an energy barrier between FTO substrate and mesoporous TiO_2 film as having a more negative conduction band edge than TiO_2. This energy barrier not only reduced the electron back transfer from FTO to I_3^- in the electrolyte, but also resulted in the accumulation of photogenerated electrons, which increased the electron density in the conduction band of TiO_2. Therefore, the device based on FTO/ZCF substrate achieved a remarkably enhanced V_{oc}, FF, and energy conversion efficiency, compared to that of device employing bare FTO and FTO/TCF. These results were confirmed by the EIS analysis and OCVD technique. Therefore, we investigated the different effects of ZCF and TCF to photoelectron conversion process, and demonstrated a different mechanism of compact film to improve the photovoltage performance of DSSCs.

Acknowledgements

We acknowledge the financial support of the Ministry of Science and Technology of China through Hi-Tech plan (Funding No. 2006AA03Z347), and the partial financial support from the National Nature Science Foundation of China (50125309), National Basic Research Program of China (No. 2011CB933300), National Science Fund for Talent Training in Basic Science (Grant No. J0830310) and the PhD Research Foundation of Wuhan University (20102020201000016). We also acknowledge the help of the Nanoscience and Nanotechnology Center at Wuhan University for the SEM and UV–vis spectrophotometer characterization.

References

[1] B. O'Regan, M. Gratzel, Nature 353 (1991) 737–740.
[2] H. Chang, K.C. Cho, C.G. Kuo, M.J. Kao, K.D. Huang, K.H. Chu, X.P. Lin, J. Alloys Compd. 509 (2011) S486–S489.
[3] S.J. Wu, H.W. Han, Q.D. Tai, J. Zhang, B.L. Chen, S. Xu, C.H. Zhou, Y. Yang, H. Hu, X.Z. Zhao, Appl. Phys. Lett. 92 (2008) 122106.
[4] S.S. Kim, J.H. Yum, Y.E. Sung, J. Photochem. Photobiol. A 171 (2005) 269–273.
[5] S.J. Wu, H.W. Han, Q.D. Tai, J. Zhang, S. Xu, C.H. Zhou, Y. Yang, H. Hu, B.L. Chen, B. Sebo, X.Z. Zhao, Nanotechnology 19 (2008) 215704.
[6] T. Taguchi, X.T. Zhang, I. Sutanto, K. Tokuhiro, T.N. Rao, H. Watanabe, T. Nakamori, M. Uragami, A. Fujishima, Chem. Commun. 19 (2003) 2480–2481.
[7] S.J. Wu, H.W. Han, Q.D. Tai, J. Zhang, S. Xu, C.H. Zhou, Y. Yang, H. Hu, B.L. Chen, X.Z. Zhao, J. Power Sources 182 (2008) 119–123.
[8] E. Palomares, J.N. Clifford, S.A. Haque, T. Lutz, J.R. Durrant, J. Am. Chem. Soc. 125 (2003) 475–482.
[9] Y. Diamant, S.G. Chen, O. Melamed, A. Zaban, J. Phys. Chem. B 107 (2003) 1977–1981.
[10] S.M. Yang, Y.Y. Huang, C.H. Huang, X.S. Zhao, Chem. Mater. 14 (2002) 1500–1504.
[11] S.A. Haque, T. Park, C. Xu, S. Koops, N. Schulte, R.J. Potter, A.B. Holmes, J.R. Durrant, Adv. Funct. Mater. 14 (2004) 435–440.
[12] R. Sharma, R.S. Mane, S.K. Min, S.H. Han, J. Alloys Compd. 479 (2009) 840–843.
[13] B. Peng, G. Jungmann, C. Jager, D. Haarer, H.W. Schmidt, M. Thelakkat, Coordin. Chem. Rev. 248 (2004) 1479–1489.
[14] S. Hore, R. Kern, Appl. Phys. Lett. 87 (2005) 263504.
[15] K. Zhu, E.A. Schiff, N.G. Park, J. van de Lagemaat, A.J. Frank, Appl. Phys. Lett. 80 (2002) 685–687.
[16] H. Yu, S.Q. Zhang, H.J. Zhao, G. Will, P.B. Liu, Electrochim. Acta 54 (2009) 1319–1324.
[17] A.O.T. Patrocinio, L.G. Paterno, N.Y.M. Iha, J. Photochem. Photobiol. A 205 (2009) 23–27.
[18] S. Ito, T.N. Murakami, P. Comte, P. Liska, C. Gratzel, M.K. Nazeeruddin, M. Gratzel, Thin Solid Films 516 (2008) 4613–4619.
[19] J.B. Xia, N. Masaki, K.J. Jiang, S. Yanagida, Chem. Commun. 2 (2007) 138–140.
[20] J.B. Xia, N. Masaki, K.J. Jiang, S. Yanagida, J. Phys. Chem. C 111 (2007) 8092–8097.
[21] S. Lee, J.H. Noh, H.S. Han, D.K. Yim, D.H. Kim, J.K. Lee, J.Y. Kim, H.S. Jung, K.S. Hong, J. Phys. Chem. C 113 (2009) 6878–6882.
[22] J.H. Noh, S. Lee, J.Y. Kim, J.K. Lee, H.S. Han, C.M. Cho, I.S. Cho, H.S. Jung, K.S. Hong, J. Phys. Chem. C 113 (2009) 1083–1087.
[23] J.X. Mou, W.G. Zhang, J. Fan, H. Deng, W. Chen, J. Alloys Compd. 509 (2011) 961–965.
[24] J. Zhang, W.X. Que, Q.Y. Jia, P. Zhong, Y.L. Liao, X.D. Ye, Y.C. Ding, J. Alloys Compd. 509 (2011) 7421–7426.
[25] S.K. Sharma, A.I. Inamdar, H. Im, B.G. Kim, P.S. Patil, J. Alloys Compd. 509 (2011) 2127–2131.
[26] Y.M. Liu, X.H. Sun, Q.D. Tai, H. Hao, B.L. Chen, N. Huang, B. Sebo, X.Z. Zhao, J. Power Sources 196 (2011) 475–481.
[27] M.F. Hossain, S. Biswas, M. Shahjahan, T. Takahashi, J. Vac. Sci. Technol. A 27 (2009) 1047–1051.

[28] R.L. Willis, C. Olson, B. O'Regan, T. Lutz, J. Nelson, J.R. Durrant, J. Phys. Chem. B 106 (2002) 7605–7613.
[29] S. Ito, P. Liska, P. Comte, R.L. Charvet, P. Pechy, U. Bach, L. Schmidt-Mende, S.M. Zakeeruddin, A. Kay, M.K. Nazeeruddin, M. Gratzel, Chem. Commun. 34 (2005) 4351–4353.
[30] R. Kern, R. Sastrawan, J. Ferber, R. Stangl, J. Luther, Electrochim. Acta 47 (2002) 4213–4225.
[31] L.Y. Han, N. Koide, Y. Chiba, T. Mitate, Appl. Phys. Lett. 84 (2004) 2433–2435.
[32] T. Hoshikawa, R. Kikuchi, K. Eguchi, J. Electroanal. Chem. 588 (2006) 59–67.
[33] J. Van de Lagemaat, N.G. Park, A.J. Frank, J. Phys. Chem. B 104 (2000) 2044–2052.
[34] S. Burnside, J.E. Moser, K. Brooks, M. Gratzel, D. Cahen, J. Phys. Chem. B 103 (1999) 9328–9332.
[35] F. Fabregat-Santiago, J. Bisquert, G. Garcia-Belmonte, G. Boschloo, A. Hagfeldt, Sol. Energy Mater. Sol. C 87 (2005) 117–131.
[36] F. Fabregat-Santiago, J. Bisquert, E. Palomares, L. Otero, D.B. Kuang, S.M. Zakeeruddin, M. Gratzel, J. Phys. Chem. C 111 (2007) 6550–6560.
[37] M. Adachi, M. Sakamoto, J.T. Jiu, Y. Ogata, S. Isoda, J. Phys. Chem. B 110 (2006) 13872–13880.
[38] J. Bisquert, A. Zaban, M. Greenshtein, I. Mora-Sero, J. Am. Chem. Soc. 126 (2004) 13550–13559.
[39] A. Zaban, M. Greenshtein, J. Bisquert, Chemphyschem 4 (2003) 859–864.
[40] D. Cahen, G. Hodes, M. Gratzel, J.F. Guillemoles, I. Riess, J. Phys. Chem. B 104 (2000) 2053–2059.